Pharm Res (2013) 30:670–682
DOI 10.1007/s11095-012-0904-4

RESEARCH PAPER

Protected Graft Copolymer Excipient Leads to a Higher Acute Maximum Tolerated Dose and Extends Residence Time of Vasoactive Intestinal Peptide Significantly Better than Sterically Stabilized Micelles

Sandra Reichstetter • Gerardo M. Castillo • Israel Rubinstein • Akiko Nishimoto-Ashfield • ManShun Lai • Cynthia C. Jones • Aryamitra Banjeree • Alex Lyubimov • Duane C. Bloedow • Alexei Bogdanov Jr. • Elijah M. Bolotin

Received: 17 May 2012 / Accepted: 8 October 2012 / Published online: 7 December 2012

ABSTRACT

Purpose To determine and compare pharmacokinetics and toxicity of two nanoformulations of Vasoactive Intestinal Peptide (VIP).

Methods VIP was formulated using a micellar (Sterically Stabilized Micelles, SSM) and a polymer-based (Protected Graft Copolymer, PGC) nanocarrier at various loading percentages. VIP binding to the nanocarriers, pharmacokinetics, blood pressure, blood chemistry, and acute maximum tolerated dose (MTD) of the formulations after injection into BALB/c mice were determined.

Results Both formulations significantly extend *in vivo* residence time compared to unformulated VIP. Formulation toxicity is dependent on loading percentage, showing major differences between the two carrier types. Both formulations increase *in vivo* potency of unformulated VIP and show acute MTDs at least 140 times lower than unformulated VIP, but still at least 100 times higher than the anticipated highest human dose, 1–5 μg/kg. These nanocarriers prevented a significant drop in arterial blood pressure compared to unformulated VIP.

Conclusions While both carriers enhance *in vivo* residence time compared to unformulated VIP and reduce the drop in blood pressure immediately after injection, PGC is the excipient of choice to extend residence time and improve the safety of potent therapeutic peptides such as VIP.

KEY WORDS long-acting vasoactive intestinal peptide · maximum tolerated dose · nanocarrier · protected graft copolymer · sterically stabilized micelles

ABBREVIATIONS

MRT	mean residence time
MTD	maximum tolerated dose
PGC	protected graft copolymer
PK	pharmacokinetics
SSM	sterically stabilized micelles
VIP	vasoactive intestinal peptide

INTRODUCTION

Vasoactive intestinal peptide (VIP) is a 28 amino-acid neuropeptide that is expressed in a variety of cells in the CNS, the gastrointestinal tract, and other tissues, and exhibits potent vasodilatory and immunomodulatory effects (1,2). Therapeutic efficacy of VIP has been demonstrated in a number of models of inflammatory diseases in rodents: e.g. VIP prevents and ameliorates collagen-induced arthritis

S. Reichstetter • G. M. Castillo • A. Nishimoto-Ashfield • M. Lai • C. C. Jones • E. M. Bolotin (✉)
PharmaIN Corp., 19805 N. Creek Parkway
Bothell, Washington 98011, USA
e-mail: ebolotin@pharmain.com

I. Rubinstein
College of Medicine, The University of Illinois
840 S. Wood St. (M/C 719) 920-N CSB
Chicago, Illinois 60612, USA

I. Rubinstein
Jesse Brown VA Medical Center
Chicago, Illinois 60612, USA

A. Banjeree • A. Lyubimov
College of Medicine, The University of Illinois
808 S. Wood Street, Rm. 1306
Chicago, Illinois 60612, USA

D. C. Bloedow
School of Pharmacy, The University of Washington
H-272, Box 357610
Seattle, Washington 98195-7631, USA

A. Bogdanov Jr.
University of Massachusetts Medical School
Worcester, Massachusetts, USA

(5–8) and improves survival in models of septic shock in mice (9,10). It has also shown promise in the treatment of experimental autoimmune encephalitis (EAE, a rodent model of multiple sclerosis) (11–13).

The mechanism of VIP-mediated immunomodulation is believed to stem from the fact that VIP can induce regulatory T-cells (Treg) and that it creates an environment that favors the differentiation of Type 2 T-helper cells (Th2) that mainly produce interleukin (IL)-4 and IL-10 cells over Th1-cells which produce IFN-γ and Th17-cells which produce IL-17 (5,6,11,14–19). This change of environment induces the anti-inflammatory activity in the context of the Th1/Th17 dominated T-cell response that is seen in most of the organ-specific chronic inflammatory diseases (5,6,11,14–19). Unfortunately, the potential therapeutic use of VIP in patients with various autoimmune diseases is hampered by serious limitations. Exogenous VIP disappears quickly from the blood, undergoing rapid degradation and inactivation. In fact, after i.v. infusion of unformulated VIP into healthy human volunteers, VIP is cleared with a half-life of about one minute (20). To ensure a detectable serum level, which is presumed to be necessary for the peptide to be effective, higher doses or long-term intravenous infusions of VIP would have to be used. This, in turn, could lead to a precipitous decrease in systemic arterial pressure and tachycardia, flushing, and diarrhea (20,21), thereby limiting its use in humans. These issues need to be solved before VIP can be used as a commercial immunotherapeutic drug. Here, two different nanocarrier formulations, one polymer-based, called protected graft co-polymer (PGC, Fig. 1a), and one micellar, called sterically stabilized micelles (SSM, Fig. 1b), are compared in their ability to improve safety and to extend residence time in the body upon injection. The Maximum Tolerated Dose (MTD) of both formulations is primarily the function of drug:nanocarrier weight ratio or loading, with very different patterns for PGC and SSM. We demonstrated that both nanocarrier formulations are very efficient in increasing the potency of unformulated VIP: both PGC and SSM lower the acute MTD at least 140 times compared to unformulated VIP while simultaneously reducing the blood pressure decreasing activity of unformulated VIP. After subcutaneous injection, both formulations achieve MTDs in mice that are at least 100 times higher than the anticipated human dose of 1-5 μg/kg.

MATERIALS AND METHODS

PGC Carrier Synthesis

PGC was synthesized as described by Castillo *et al.* (4). Specifically, a 20PLL solution was prepared by dissolving 0.46 g 20 kDa Poly-l-lysine (20PLL, SAFC, St. Louis MO) in 10 ml of 0.23 M 4-(2-hydroxyethyl)-1-piperazineethanesulfonic acid (HEPES, Fisher Scientific, Waltham MA) in water. The pH was adjusted to pH=7.8 using NaOH (Fisher Scientific, Waltham MA) and the solution was placed on ice. A solution of 5.4 g of Methoxy-PEG-carboxymethyl (MPEG-CM, Mw=5000; Laysan Bio, Arab AL) in 20 ml degassed water was prepared. A 1.15x molar excess of N-hydroxysuccinimide-sulfate (NHSS, ChemPep, Wellington FL) over carboxyl groups was added to MPEG-CM, and, once dissolved, a 2x molar excess of 1-ethyl-3-[3-dimethylaminopropyl] carbodiimide HCl (EDC, Sigma, St. Louis MO) over carboxyl groups was added while stirring and the activation was allowed to proceed for 15 minutes. The activated MPEG-CM was added to the 20PL solution, the pH was adjusted to pH7.4–7.8 with NaOH and allowed to react at room temperature for a total of four hours. Analysis of free amino groups by TNBS assay (2,4,6-trinitrobenzenesulfonic acid, Fluka, St. Louis MO) as previously described (22), as a measure of PLL amino groups acylation with PEG side chains. The assay indicated approximately 50% PEG modification. The solution was then lyophilized and dissolved in 60 ml dichloromethane (DCM, Fluka, St. Louis MO). After centrifugation at a relative centrifugal force (RCF) of 22,000×g to remove any precipitates, the supernatant was collected and the pellet was washed with another 20 ml DCM and re-centrifuged. This second supernatant was pooled with the first supernatant. A 5x molar excess of N,N-diisopropylethylamine (DIPEA, Acros, Morris Plains NJ) over the remaining amino groups was added while stirring and C18-NHS (synthesized according to the method of Lapidot *et al.* (23)) was added at a molar ratio of 3:1 over the remaining amino groups. The reaction was allowed to proceed overnight at room temperature. An aliquot of reaction mixture was dried, dissolved in water, and free amino groups were assayed using the TNBS test to confirm the completeness of acylation. The material was rotary evaporated to dryness and dissolved in 100 ml ethanol and washed with 10 volume changes of 80% ethanol and another 10 volume changes of water using an ultrafiltration cartridge with 100 kDa molecular weight cut-off. The resulting PGC sample was filtered using a 0.2 μm filter and lyophilized (Fig. 2).

PGC carrier molecules have a hydrodynamic diameter of approximately 17–22 nm (measured using Ultrahydrogel (TosoH G4000PWXL, 7.8 mm×30 cm) gel-permeation chromatography calibrated with protein standards of known hydrodynamic diameters) with a calculated molecular weight of 360 kDa.

Formulation with VIP

PGC-VIP

One mg of VIP was dissolved in 1 ml water and mixed with enough PGC carrier in water (at concentration equal to or less

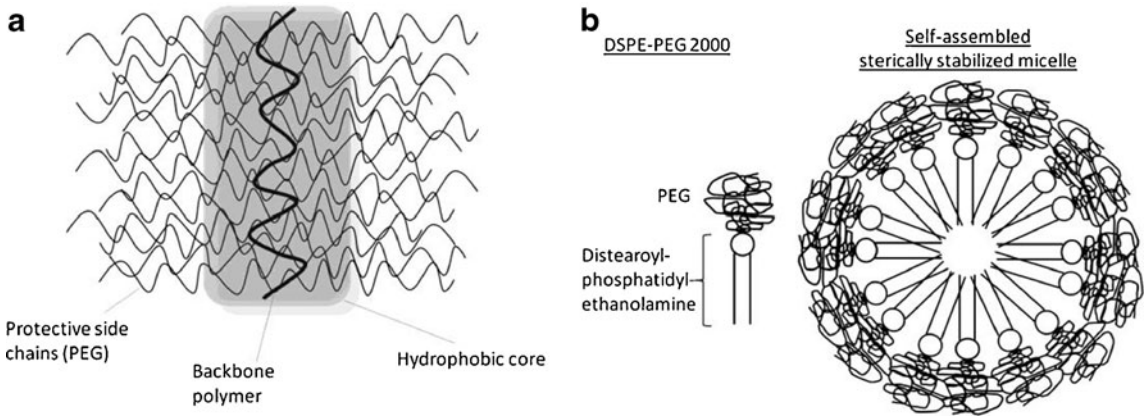

Fig. 1 Schematic depiction of PGC (**a**) and SSM (**b**) nanocarriers. PGC is about 17–22 nm in size (3,4); SSM about 15 nm.

than 50 mg PGC/ml) to obtain VIP:carrier weight ratios of 0.08%, 0.5%, 0.75%, 1%, and 2%. The mixtures were incubated for 2 h at room temperature and lyophilized.

SSM-VIP

For consistency, we identify our formulations using the formula "nanocarrier-load molecule". Consequently, the VIP formulation is named SSM-VIP although it has been called "VIP in SSM" or VIP-SSM previously (24,25). The formulation of VIP using micelles (SSM-VIP) was performed as previously described (25). Briefly, 1000 mg of PEGylated distearoyl phosphatidylethanolamine (DSPE-PEG2000) (Lipoid, Ludwigshafen, Germany) was dissolved in 45 ml saline and incubated at room temperature in the dark for 60 min. One mg of VIP was dissolved in 1 ml saline and mixed with enough DSPE-PEG 2000 to yield carriers loaded with VIP at weight ratios of 0.08%, 0.5%, 0.75%, 1%, and 2%. The mixtures were incubated for 2 h at room temperature and lyophilized.

Binding Studies and Determination of the Dissociation Constant (Kd)

VIP was mixed with a fixed amount of PGC (0.6 mg at 2.4 mg/ml final concentration) or SSM carriers (0.5 mg at 2 mg/ml final concentration) at concentrations between 72 μM and 188 μM in the PGC mixtures and between 120 μM and 240 μM in the SSM mixtures in an aqueous solution of 100 mM NaCl (Fisher Scientific, Waltham MA) and 100 mM HEPES (Fisher Scientific, Waltham MA) in quadruplicate. The mixtures were incubated for 2 h at room temperature. The mixtures were subjected to ultrafiltration using 100 kDa MWCO cellulose membrane centrifuge filter (Amicon Ultra Ultracel 100 k, Millipore, Billerica MA) by centrifuging at 18,000×g for 12 min. This filter retains the carrier and VIP that is bound to the carrier. Free VIP in the filtrate was analyzed using HPLC (Waters, Milford MA). The following HPLC protocol was used: Solvent A: 5% acetonitrile (Fisher Scientific, Waltham MA) in water with 0.1% trifluoroacetic acid (TFA, Fisher Scientific, Waltham MA); Solvent B:

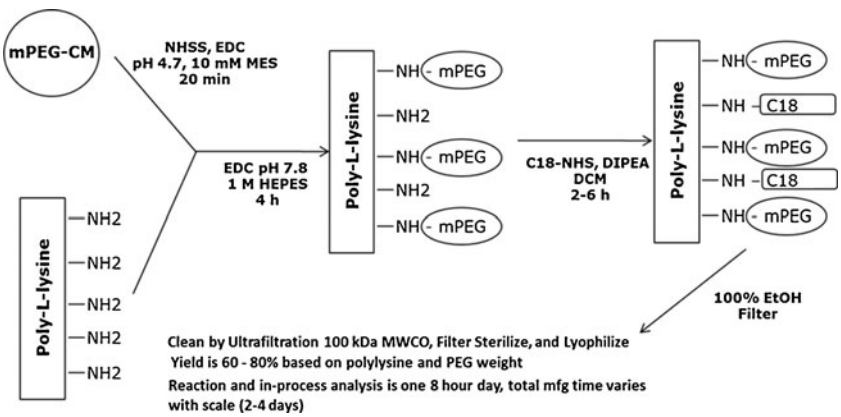

Fig. 2 Schematic depiction of PGC carrier synthesis.

100% Acetonitrile with 0.1% TFA. Column: Synergi 2.5 um Max-RP (20×4 mm) 100 Å beads, Mercury (Phenomenex, Torrance CA); 1.5 ml/min; 50 µl injection. Gradient: 0.0–0.5 min: 0%B - 0%B; 0.5–1.0 min: 0%B–10%B, 1.0–5.0 min: 10%B–50%B; 5.0–5.5 min: 50%B–99%B, 5.5–6.0 min 99%B–0%B. Monitoring and quantitation was performed at 220 nm, retention time: 3.0 min. A standard was used for quantitation of peak area under the curve (AUC). Two independent binding experiments were done for both the PGC-VIP and the SSM-VIP formulations. The dependence of [VIP_{bound}] from [Free VIP] was plotted at a constant PGC or SSM concentration of 2.4 mg/ml and 2 mg/ml, respectively (Fig. 3) and a nonlinear regression curve fit for each was performed using GraphPad Prism (GraphPad Software Inc., San Diego CA) for determining B_{max}, R^2, and K_d (26,27).

Pharmacokinetics Studies

Animals and Blood Sampling

Female BALB/c mice, 4 to 5 weeks old, were purchased from Charles River Laboratories (Wilmington MA). The animals were housed in a Specific Pathogen Free (SPF) facility at 12 h/12 h light/dark cycle and had access to food and water *ad libitum*. For the pharmacokinetics (PK) studies, the mice were separated into 3 groups of 25 mice. Each group was injected subcutaneously (SC) with 100 µg/kg VIP, either free or formulated with SSM or PGC at 0.5% loading. At each time point 200 µl blood was drawn under isoflurane anesthesia by retro-orbital bleed from 5 mice/group. Each mouse provided two sampling time-points and was euthanized after the second blood draw. Five mice in each group were sampled at t= 30 min and 6 h, five were sampled at 1 h and 9 h, five at 2 h and 12 h, five at 4 h and 24 h, and five at 48 h and 72 h, so that the time points combined were t=30 min, 1, 2, 4, 6, 9, 12, 24, 48, and 72 h. Pooled serum of 10 age-matched BALB/c mice was tested in quadruplicate as background control. Blood was collected into serum collection micro-tubes with gel separator (Becton Dickinson, Franklin Lakes NJ) containing 2 µl of a premixed protease inhibitor cocktail (Set I, Calbiochem, La Jolla CA).

ELISA

VIP concentrations in the serum samples were determined by an extraction-free, competitive ELISA according to the manufacturer's instructions (Bachem, Torrance CA). The VIP standard included in the kit was used to create the standard curve. The samples from mice that were injected with formulated VIP were diluted 1:5 with sample dilution buffer from the ELISA kit. Serum samples from mice injected with free VIP were assayed undiluted.

Serum from the 9 h time point of mice injected with PGC-VIP and the 20 min time point of mice injected with unformulated VIP were diluted 1:3 with sample dilution buffer from the ELISA kit. Then 120ul of this dilution was filtered through 100 kDa MWCO filters, as in the binding study above. 50ul of the filtrate and 50ul of the unfiltered 1:3 diluted serum were used in a VIP ELISA, as described above.

PK Data Analysis

PK serum profiles were analyzed using standard non-compartmental analysis to determine: maximum concentration (C_{max}), time of maximum concentration (T_{max}), area under the concentration-time profile from time 0 until the last detectable concentration ($AUC_{0\ to\ last}$), area under the concentration-time profile from time 0 extrapolated to infinite time ($AUC_{0\ to\ infinity}$), terminal half-life, and MRT. In estimating the areas under the curve, the linear trapezoidal or logarithmic trapezoidal rules were used for increasing concentrations or decreasing concentrations, respectively. Terminal slopes for calculation of terminal half-life were estimated using $1/Y^2$ weighting.

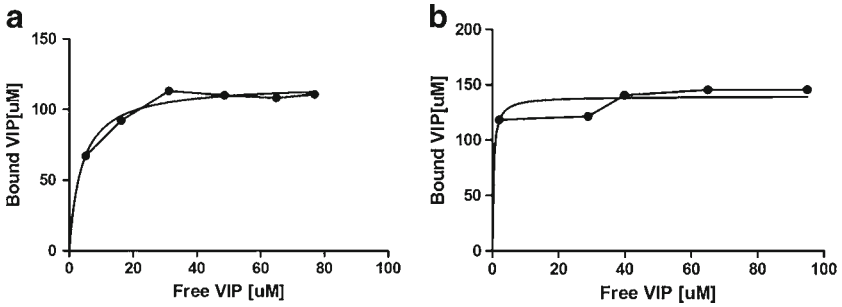

Fig. 3 VIP binding in 100 mM NaCl, 100 mM HEPES at a carrier concentration of 2.4 mg/ml for PGC and 2.0 mg/ml for SSM (**a**) PGC-VIP, (**b**) SSM-VIP. The experiment was done in quadruplicate; free VIP was separated from bound by ultrafiltration, VIP quantitation was by HPLC. The exponential association, one-phase fit non-linear regression method was used for data fitting using GraphPad Prism (GraphPad Software Inc., San Diego CA).

Blood Pressure Measurements

Arterial blood pressure was measured using a non-invasive tail-cuff measuring device (Kent Scientific, Torrington CT). Ten blood pressure values before and twenty values starting 5 min after injection of VIP formulations were measured and compared using Student's T-test.

Determination of Acute Maximum Tolerated Dose (MTD)

Four mice were injected with a 2% loading VIP formulation (SSM or PGC) at a dose of 50 μg/kg. If the mice survived the following 24 h, another set of mice was injected with 100 μg/kg of the same formulation. At doses above 100 μg/kg the dosing increase to find the MTD after mice survived the previous dose was by increments of 100 μg/kg. If the mice survived a dose of 1000 μg/kg, the next higher dose was 1250 μg/kg, and 1500 μg/kg thereafter. Once MTD was established for a higher loading percentage, this dose was used as starting point for the next lower loading percentage to be tested. For unformulated VIP, a starting dose of 50 mg/kg was used and doses were increased by a factor 2 until a dose was found that was not safe. To measure MTD more precisely the dose corresponding to an average of the highest tested safe dose, and the lowest lethal dose was tested next (i.e. if lethality was observed at 200 mg/kg, but none at 100 mg/kg, 150 mg/kg was tested next, and 175 mg/kg thereafter).

Clinical Chemistry

Clinical Chemistry parameters were measured in the mice serum samples using an Olympus AU400 Clinical Chemistry Analyzer by the following methods: Urea Nitrogen (BUN) - Modified urease technique (28); Creatinine - Jaffe method (29); Total Protein - Biuret technique (30–32); Albumin - Bromocresol green method (33–35); Aspartate Aminotransferase (AST/GOT) - Modified Karmen procedure (36); Alanine Aminotransferase (ALT/GPT) - Modified Wroblewski & La Due procedure (37); and Total Bilirubin - Modified Walters and Gerard method (38). Values of PGC-VIP and SSM-VIP treated animals were compared to saline treated and age-matched, untreated animals, and statistical significance was evaluated using Student's T-test.

Cardiotoxicity Markers

Serum concentration of cardiac troponin I (cTnI), skeletal troponin I (sTnI), and Myosin light chain 3 (Myl3) were measured using a validated procedure on the Meso Scale Discovery (MSD) platform according to manufacturer's instructions (MSD, Gaithersburg MD). Values from PGC-VIP- and SSM-VIP-treated animals were compared to saline-treated and to age-matched, untreated animals; P values were obtained using Student's T-test with P values less than 0.05 considered significant.

Data and Statistical Analyses

Data are expressed as mean +/-SD where appropriate. Values from PGC-VIP- and SSM-VIP-treated animals were compared to saline-treated and to age-matched, untreated animals; P values were obtained using Student's t-test with P values less than 0.05 considered significant.

RESULTS

Formulation of VIP with either PGC, that gave PGC-VIP complex, or DSPE-PEG 2000, to obtain sterically stabilized micelles (SSM-VIP), resulted in nanocarrier-VIP complexes with a measurable binding constant that suggested binding of VIP to the nanocarriers. The dissociation constant (K_d) of VIP from nanocarrier was in the range between 3.9 μM (95% confidence interval (CI): 1.8 μM to 5.9 μM) and 4.1 μM (95% CI: 0.07 μM to 8.1 μM). The binding maximum (B_{max}) was calculated as between 21.35 nmol/mg (95% CI: 16.99 to 25.71 nmol/mg) and 49.2 nmol/mg (95% CI: 45.3 to 53.2 nmol/mg) or 7–18 VIP molecules per PGC molecule based on the calculated PGC molecular weight of 360 kDa. The concentration of free VIP in equilibrium rose steadily with increasing VIP:PGC weight ratio in the formulation (Fig. 3a). SSM-formulations showed a sigmoidal curve with a large increase in the free VIP fraction at higher loading ratios (Fig. 3b). This behavior made it more difficult to calculate the K_d accurately and lead to a K_d that had a considerably larger error than that calculated for PGC-VIP. The K_d of VIP binding to SSM was in the range between 0.4 μM (95% CI: 0 μM to 1.238 μM) and 0.9 μM (95% CI: 0.23 to 1.56 μM). The B_{max} was calculated to be in the range between 69.8 nmol/mg (95% CI: 60.5 to 79.1 nmol/mg) and 75.92 nmol/mg (95% CI: 70.72 to 81.12 nmol/mg). Based on the previously reported micelle aggregation number of approximately 93 in HEPES buffered saline (39), which corresponds to a micelle with a molecular weight of around 258 kDa, and a binding capacity of 18–20 VIP molecules per micelle. Other groups have reported a micelle aggregation number of 72 +/−10% (40), which suggests a molecular weight of 200 kDa, and a VIP binding capacity between 14 and 15 VIP molecules per micelle. Calculations of B_{max} and K_d using Scatchard plot lead to very similar values for both PGC and SSM formulations of VIP (data not shown).

Pharmacokinetic (PK) properties were determined for unformulated VIP and VIP-nanocarrier formulations with

0.5% loading following SC injection at a dose of 100 μg VIP /kg in five mice per group (Fig. 4 and Table I). VIP levels in serum were tested using a competitive ELISA (Bachem, Torrance CA). The assay was able to detect VIP in serum in the presence or absence of PGC or SSM at equal sensitivity, i.e. it does not differentiate between formulated and free VIP (data not shown). After SC injection of PGC-VIP in BALB/c mice, measured blood VIP-levels demonstrated markedly improved pharmacokinetics compared to those in animals given SSM-VIP or unformulated VIP. Following SC injection of PGC-VIP, VIP was detectable at 2 h after injection, peaked at 4 h (=T_{max}), and was detectable for at least 48 hours, with a corresponding MRT of 11.2 h. After SC injection of SSM-VIP, VIP serum concentrations peaked earlier (T_{max}=2 h) and VIP disappeared from the serum more quickly compared to PGC-VIP (detectable for only 4 hours with a MRT of 2.63 h). In contrast, serum concentrations of free VIP after SC injections dropped off very quickly, demonstrating the challenges of using unformulated VIP clinically in humans. Serum VIP concentrations increased very rapidly (T_{max} 0.5 h) but were detectable for only 60 min, as evidenced by a very short MRT (0.520 h). The body exposure to the detectable blood level of VIP was much greater for PGC-VIP ($AUC_{0\ to\ infinity}$ 218 ng/ml×h) compared to SSM-VIP ($AUC_{0\ to\ infinity}$ 0.294 ng/ml×h) and unformulated VIP ($AUC_{0\ to\ infinity}$ 12.0 ng/ml×h). To determine whether at least a part of PGC-VIP travels intact from the injection site to the blood stream, serum of mice injected with unformulated VIP and PGC-VIP were collected, from time points where high VIP serum-concentrations were detectable, and filtered through 100 kDa MWCO filters that retain PGC-VIP but not free VIP. The resulting filtrates were tested in the VIP ELISA. Using serum from mice injected with PGC-VIP, 15 times more VIP was retained in the filter compared to serum from mice injected with unformulated VIP (data not shown).

Blood pressure measurements revealed that formulation of VIP with either SSM or PGC increased the dose at which a significant decrease in arterial blood pressure occurs from approximately 2.5 μg/kg with unformulated VIP to doses between 50 and 800 μg/kg depending on the loading percentage of the formulation, with higher doses at lower loading percentages (Table II).

Table I Pharmacokinetic Parameters of SC Injected Unformulated VIP, PGC-VIP, and SSM-VIP in BALB/c Mice (n=5, dose 100 μg/kg)

	PGC-VIP	SSM-VIP	Unformulated VIP
T_{max} (h) [a]	4.0	2.0	0.5
C_{max} (ng/mL) [b]	16.2	0.100	36.6
$AUC_{0\ to\ last}$ (ng/mL × h)	218	0.244	12.0
$AUC_{0\ to\ infinity}$ (ng/mL × h)	218	0.294	12.0
Mean Residence Time (h)	11.2	2.63	0.520
Terminal Half-Life (h)	4.24	1.15	0.431

[a] T_{max}: Time point of maximal serum concentration [b] C_{max}: highest serum concentration measured. AUC: area under the curve

Acute MTD, the highest dose that did not cause any deaths within 24 h of dosing, was determined with SSM-VIP and PGC-VIP formulations (Fig. 5) at different loading percentages (weight VIP per weight carrier). There was an inverse correlation between the MTD and the loading percentage of the formulations. The highest MTD for SSM-VIP was 600 μg VIP/kg, at 0.5% loading, while the MTD of PGC-VIP was 1250 μg VIP/kg, at 0.75% loading (Fig. 5). The MTD as a function of loading percentage for SSM-VIP showed a steady decline with a MTD of 500 μg VIP/kg at 1% loading, 400 μg VIP/kg at 2%, and 25 μg VIP/kg at 3% loading. The curve for PGC-formulated VIP had a sigmoidal shape with a plateau at 1250 μg VIP/kg for the formulations with 0.08%, 0.5% and 0.75% loading, and a sharp decline thereafter; the MTD for 1% loading was determined as 100 μg VIP/kg and 50 μg VIP/kg for 2% loading with VIP. The PGC carrier alone did not cause acute symptoms or death in similar experiments (data not shown). The MTD of unformulated VIP was determined at 175 mg/kg. There is variability in the acute MTD between different species with rats being more tolerant to PGC-VIP (at least 1 mg/kg at 2% loading).

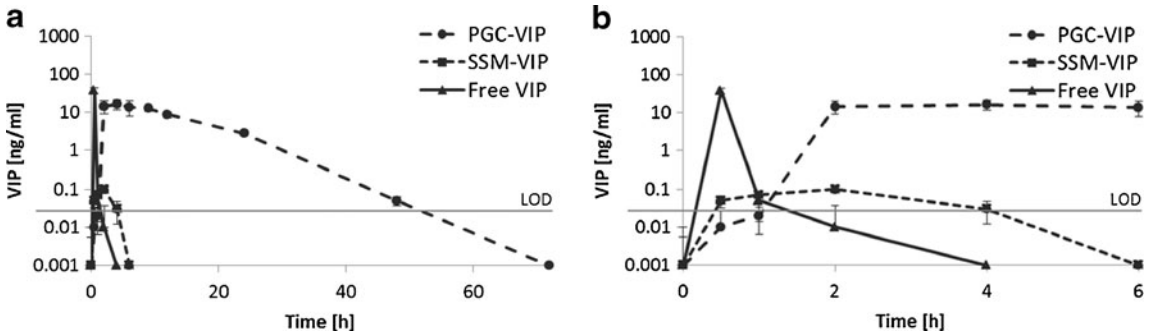

Fig. 4 Pharmacokinetics of VIP after SC injection of 100 μg/kg in BALB/c mice (n=5). (**a**) Overview of entire 72 h sampling period, (**b**) the first 6 h shown in detail. VIP quantitation in serum samples was by competitive ELISA. LOD: level of detection.

A chronic toxicity study of the 0.5% loading VIP formulations was performed using 50% of the acute MTD dose (625 μg VIP/kg for PGC-VIP at 0.5% loading and 300 μg VIP/kg for SSM-VIP at 0.5% loading). Since acute MTD is a function of loading, we chose loading of 0.5% for PGC-VIP and 0.5% loading for SSM-VIP because these loading percentages show high acute MTDs within the plateau of the function that plotted loading percentage *vs.* acute MTD (Fig. 5). The formulations were given SC three times per week for four weeks in BALB/c mice (n=5). Five more mice per group were treated identically for eight weeks. No deaths occurred in the saline or PGC-VIP groups. One mouse in the SSM-VIP groups was found dead after four weeks of treatment however it was not possible to determine the cause of death. No significant difference in weight gain compared to the saline group was detected (Fig. 6). Several clinical chemistry parameters that can signify liver or kidney toxicity did not show a significant difference compared to saline treated or age-matched untreated mice after four or eight weeks of treatment (Table III and Table IV). There was also no evidence of cardiotoxicity (Table V). Histological examination of lung, heart, liver, kidney, spleen, and brain did not show any pathologic changes (data not shown). Skin from the injection site showed minimal subcutaneous mononuclear infiltrates in the PGC-VIP and saline groups, and minimal to mild infiltrates in the SSM-VIP group (Table VI). Minimal to mild fibroplasia was found in the saline group, while fibroplasia was mild in the SSM-VIP, and mild to moderate in the PGC-VIP group. A summary of the findings at the injection site is shown in Table VI.

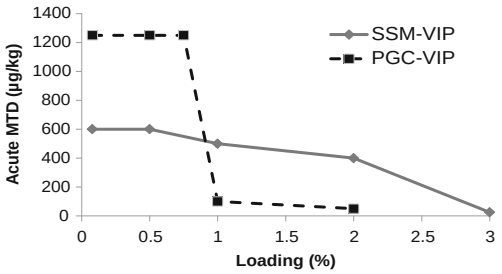

Fig. 5 Acute MTD of SSM-VIP and PGC-VIP formulations as function of loading percentage.

Table II Changes in Arterial Blood Pressure After SC Injection of Unformulated VIP, SSM-VIP, and PGC-VIP at Various Loading Percentages

Formulation	Dose [μg/kg]	Systolic BP decrease [mm Hg]	p-value (BP before *vs* after injection)
Unformulated VIP [a]	2.0	−4.8 [b]	0.078 [c]
Unformulated VIP	2.5	**19.3**	**<0.001**
PGC-VIP 0.08% loading	600	−2	0.6821
PGC-VIP 0.08% loading	800	**20**	**0.0003**
PGC-VIP 0.5% loading	400	1	0.7368
PGC-VIP 0.5% loading	600	**15**	**<0.0001**
PGC-VIP 0.75% loading	100	**11**	**0.0007**
PGC-VIP 1% loading	100	**19**	**<0.0001**
PGC-VIP 2% loading	50	**20**	**<0.0001**
SSM-VIP 0.08% loading	600	0	1
SSM-VIP 0.08% loading	800	**15**	**<0.0001**
SSM-VIP 0.5% loading	600	**13**	**0.0053**
SSM-VIP 0.5% loading	100	**11**	**0.0029**
SSM-VIP 1% loading	500	**43**	**<0.0001**
SSM-VIP 2% loading	400	**13**	**0.0005**

[a] The doses used correspond to the MTD (PGC-VIP, 1% and 2% loading, SSM-VIP 1% and 2%). For PGC-VIP 0.08 and 0.5%, and SSM-VIP 0.08% the highest dose that did not show a significant blood pressure drop, and the lowest dose that did, are shown. The lowest tested dose of SSM-VIP (0.5%, 100 μg/kg) is also shown for comparison. Each group size was n=4, except for unformulated VIP, where it was n=8. [b] negative values denote a blood pressure (BP) increase after injection compared to pre-injection levels. [c] significant results are given in bold

DISCUSSION

Inhaled VIP is being explored for the treatment of chronic obstructive pulmonary disease (COPD) (41) and for the treatment of pulmonary arterial hypertension (PAH) (42–44), including Phase II clinical trials with VIP for PAH (source: mondobiotech.com). VIP has also shown promise in the treatment of a number of inflammatory diseases in animal models (6–13,17). However, injection of unformulated VIP into humans is hampered by serious limitations such as a half-life of about one minute and effects such as a decrease in systemic arterial pressure, tachycardia, flushing, and diarrhea at a low dose of continuous infusion such as 11 $ng_{*}kg^{-1}{}_{*}min^{-1}$ or 15.8 $\mu g_{*}kg^{-1}{}_{*}day^{-1}$ (20). VIP binds to its receptor in the smooth muscle cells of blood vessels (VPAC2) which causes vasodilation (45). Since smooth muscle lies distal of the basal membrane, VIP has to extravasate to cause this effect (Fig. 7a). The receptors responsible for immunomodulatory function of VIP, VPAC1, and VPAC2 are expressed on various immune cells like T-cells and macrophages (46,47). To act on these, VIP has to be available in the bloodstream and in the inflammation site (Fig. 7b).

Due to the leaky vasculature that is present in the site of inflammation, carriers of the size of PGC and SSM passively accumulate in these sites through the enhanced permeability and retention (EPR) effect (48–51). A nanocarrier drug delivery system, with high affinity of VIP binding to a carrier (to keep it bound in circulation), that is too big to extravasate in healthy vasculature might therefore be able to improve the dangerous adverse reaction of VIP, significant drop in blood pressure, while it is expected to retain its immunomodulatory properties if the formulation is small enough to extravasate at the sites of increased vascular permeability that exist in inflammation (Fig. 7c and d).

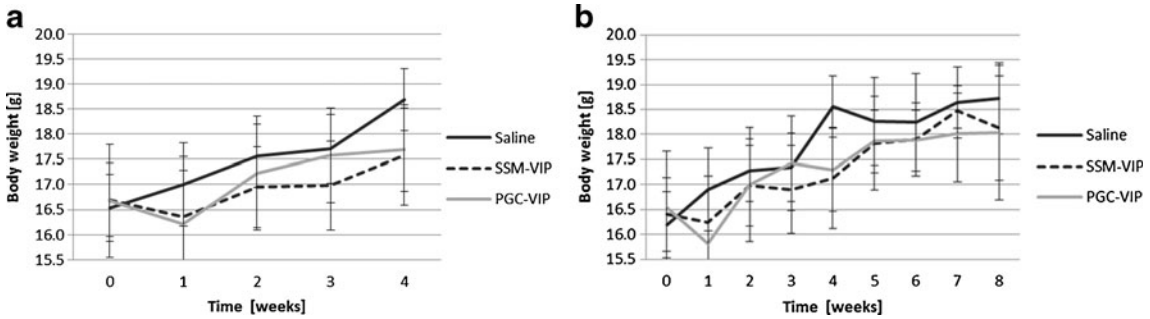

Fig. 6 Body weight of mice during 4 (**a**) and 8 (**b**) week toxicity study. Mice were treated three times per week by SC injection with 50% of the acute MTD of PGC-VIP at 0.5% loading (625 μg/kg) and SSM-VIP at 0.5% loading (300 μg/kg). A control group was SC injected with an equal volume of vehicle (saline) three times per week. A and B show different sets of mice (n=5, for SSM-VIP in B: n=4).

In addition, if the carrier sequesters VIP from enzyme-mediated inactivation in serum and prevents kidney excretion due to its size, it also enables improvement of the PK profile. Strong binding to the carrier is necessary for both an improved PK profile as well as the decrease of toxic effects such as blood pressure lowering by free VIP injections. In order to allow for the formulation of VIP with a reasonable amount of carrier, the binding capacity is also highly important. Our binding studies of VIP to the PGC carrier showed a K_d of about 3.9–4.1 μM, suggesting binding strong enough to achieve an improved PK profile and toxicity while being able to release enough free VIP to be biologically active. It also implied the existence of about 7-18 binding sites per carrier molecule. The K_d that was determined for SSM had a greater error and suggested stronger binding between 0.4 μM and 0.9 μM. Binding sites in the SSM were calculated to be about 14–20 per micelle. These values were encouraging for us, so we tested both SSM and PGC formulations of VIP for PK and toxicity as the first *in vivo* steps.

The pharmacokinetic study in mice demonstrated a marked improvement in MRT and exposure (AUC) *in vivo*, with the MRT of VIP formulated with SSM being 2.63 h, and that of VIP formulated with PGC being 11.2 h, compared to 0.52 h for unformulated VIP. We have previously demonstrated that PGC reaches the blood stream after SC injection (4). Since the T_{max} is reached much later, AUC is much larger and MRT is much longer for PGC-VIP, compared to SSM-VIP and unformulated VIP, it reasonable to expect that PGC-VIP is slowly entering the blood stream from the SC injection site as an intact complex, similar to PGC-GLP-1 (4), thereby protecting VIP in the circulation. We also showed here that serum of mice injected with PGC-VIP contain 15-times more VIP in the form of high molecular weight structures that can be filtered out with a 100 kDa MWCO filter, compared to serum from mice injected with unformulated VIP. The most likely explanation is that these high molecular weight structures are intact PGC-VIP that traveled from the injection site to the blood stream. If VIP would bind to albumin or other serum proteins to this degree, the high molecular weight VIP structures would also be found in mice injected with unformulated VIP, which is not the case.

In the case of SSM-VIP, the T_{max} is later, MRT is longer, and the AUC is smaller, compared to unformulated VIP. One possible explanation is that there is retention of a significant fraction of SSM and tightly SSM-bound VIP at the injection site. Another possible explanation could be that as the SSM-VIP formulation slowly traffics to the blood stream, it is

Table III Clinical Chemistry Panel of BALB/c Mice Treated Three Times per Week for Four Weeks

Treatment		ALT[a]	AST	TBILI	BUN	CREAT	ALB	TP	GLOB	A/G-ratio
Saline, n=5	Average	134.6	154.2	0.3	34.0	0.0	3.0	4.7	1.7	1.8
	SD	107.5	41.3	0.1	4.9	0.0	0.1	0.2	0.1	0.1
PGC-VIP, n=5	Average	82.6	101.6	0.3	31.0	0.0	2.7	4.3	1.6	1.7
	SD	47.0	27.9	0.1	3.7	0.0	0.1	0.2	0.2	0.2
SSM-VIP, n=5	Average	134.8	155.2	0.4	35.0	0.0	2.9	4.6	1.7	1.7
	SD	116.5	70.8	0.1	2.4	0.0	0.1	0.2	0.1	0.1
Untreated, n=3	Average	42.7	80.0	0.3	34.7	0.0	3.0	4.6	1.6	1.8
	SD	12.9	28.8	0.1	1.2	0.0	0.1	0.1	0.0	0.0

[a] *ALT* alanine transaminase, *AST* aspartate transaminase, *TBILI* total bilirubin, *BUN* blood urea nitrogen, *CREAT* creatinine, *ALB* albumin, *TP* total protein, *GLOB* globulin, *A/G-ratio* Albumin/globulin. SC injection for four weeks with saline, 625 μg/kg PGC-VIP, and 300 μg/kg SSM-VIP, both at 0.5% loading (all values are in ng/ml). The doses are 50% of the acute MTD. Differences between the treatment groups were not statistically significant

Table IV Clinical Chemistry Panel of Mice Treated Three Times Per Week for Eight Weeks

Treatment		ALT[a]	AST	TBILI	BUN	CREAT	ALB	TP	GLOB	A/G-ratio
Saline, *n*=5	Average	64.8	405.6	0.2	27.2	0.0	3.0	5.0	2.0	1.4
	SD	26.7	223.9	0.2	9.5	0.0	1.0	1.4	0.4	0.3
PGC-VIP, *n*=5	Average	45.6	288.0	0.0	28.0	0.0	2.1	4.0	1.9	1.2
	SD	19.9	104.3	0.0	5.7	0.0	0.5	0.1	0.6	0.5
SSM-VIP, *n*=4	Average	57.0	526.0	0.1	20.0	0.0	2.6	4.3	1.7	1.5
	SD	12.8	268.5	0.2	3.3	0.0	0.1	0.2	0.2	0.1
Untreated, *n*=3	Average	46.7	464.0	0.0	20.0	0.0	2.2	3.9	1.6	1.4
	SD	23.4	307.5	0.0	4.0	0.0	0.3	0.2	0.1	0.3

[a] *ALT* alanine transaminase, *AST* aspartate transaminase, *TBILI* total bilirubin, BUN: blood urea nitrogen, *CREAT* creatinine, *ALB* albumin, *TP* total protein, *GLOB* globulin, *A/G-ratio* Albumin/globulin. SC injection for eight weeks with saline, 625 μg/kg PGC-VIP, and 300 μg/kg SSM-VIP, both at 0.5% loading (all values are in ng/ml). Differences between the treatment groups were not statistically significant

immediately destroyed in the blood upon dilution below the Critical Micelle Concentration (CMC) which results in a release of VIP that gets rapidly eliminated. Given the fact that the binding affinity of VIP to SSM is higher than that of VIP to PGC, one would expect SSM-VIP to have a longer MRT *in vivo* compared to PGC-VIP. This, however, is not the case. Assuming similar PEG surfaces, there are two potential factors: size and stability of the carriers. Due to its larger hydrodynamic diameter compared to SSM-VIP (~15 nm), PGC-VIP (~18-22 nm) is distributed from the injection site to the blood stream at a slower rate which accounts for the delay in T_{max}. The transport of large molecules from a SC injection site into the plasma is thought to occur via the relatively slow lymphatic flow. The transport of SC-injected small molecules and proteins through the lymphatic system has been shown to depend upon the molecular weight of the drug (52). However, more research in the specific case of PGC is necessary to answer the question if indeed, and why, PGC-VIP is transported more slowly into the blood stream as compared to SSM-VIP. The slow transport of PGC-VIP from the injection site is likely to be an important factor in the extended PGC-VIP MRT compared to that for SSM-VIP and unformulated VIP (11.2, 2.63, and 0.520 h, respectively). The other important factor that plays a role in the extended MRT of PGC-VIP compared to SSM-VIP is most likely the stability of the nanocarrier. In the case of PGC, covalent bonds need to be cleaved to degrade the nanocarrier. However, SSM will disintegrate below the CMC. If and once SSM-VIP reaches the blood stream, the VIP cargo is released at a much higher rate than in the case of PGC-VIP due to the dissociation of micelles. Once VIP is free in the blood stream it will be degraded within minutes which could be the reason for a much reduced C_{max} when comparing SSM-VIP to PGC-VIP. Which one of these mechanisms is more important will have to be investigated in the future.

VIP has been shown to work as an immunomodulator by inducing T-regs and tolerogenic dendritic cells, increasing IL-10 production, inhibiting activation of nuclear factor κB (NFκB), and decreasing pro-inflammatory cytokine production (6,11,14,53–66). It is therefore possible that its continued presence in an inflammatory disease is not necessary for efficacy, and long intervals between administrations in humans might be feasible. Nevertheless, a presence at the inflammation for at least several hours is most likely beneficial, which is achievable using the PGC and, possibly, SSM formulations too. Due to the long residence time of the PGC formulation that allows VIP to be detectable at 48 h after injection, this formulation might also be suitable for at least a once per day injection in humans, if later studies show that continued presence of VIP is indeed necessary for efficacy.

Table V Cardiotoxicity Panel of Mice Treated Three Times Per Week for Four and Eight Weeks

Marker Treatment length, weeks		cTnI[a] 4	Myl3[b] 4	sTnI[c] 4	cTnI[a] 8	Myl3[b] 8	sTnI[c] 8
Saline, *n*=3	Average	0.0	0.1	4.1	104.7	58.8	9.6
	SD	0.0	0.0	2.3	75.0	46.0	3.6
SSM-VIP, *n*=5	Average	0.0	0.0	2.8	140.6	91.8	8.0
	SD	0.0	0.0	1.4	88.7	67.5	2.7
PGC-VIP, *n*=5	Average	0.0	0.0	2.5	122.8	57.6	6.3
	SD	0.0	0.0	0.5	34.5	17.7	1.4
Untreated, *n*=1		0.0	0.1	3.3	151.5	85.6	21.0
	SD	N/A	N/A	N/A	N/A	N/A	N/A

[a]cardiac troponin 1, [b]essential myosin light chain 3, [c]slow twitch cardiac troponin 1. All values are shown as ng/ml. SC injection for four weeks with saline, 625 μg/kg PGC-VIP, and 300 μg/kg SSM-VIP, both at 0.5% loading. Differences between the treatment groups were not statistically significant

Table VI Summary of Subcutaneous Mononuclear Cell Infiltrates and Fibroplasia in Injection Sites of Mice Treated Three Times Per Week for 4 Weeks

Finding	Saline $n=5$[a]	PGC-VIP 625 μg/kg $n=5$	SSM-VIP 300 μg/kg $n=5$
Mononuclear cell infiltrate	5/5	5/5	5/5
minimal	5/5	5/5	3/5
mild	0/5	0/5	2/5
Fibroplasia	5/5	5/5	5/5
minimal	4/5	0/5	0/5
mild	1/5	2/5	5/5
moderate	0/5	3/5	0/5

[a] SC injection with saline, 625 μg/kg PGC-VIP, or 300 μg/kg SSM-VIP. Differences between the treatment groups were not statistically significant

Because of the small hydrodynamic diameters of both PGC and SSM, both formulations with VIP are able to accumulate in areas with increased vascular permeability as a result of the EPR effect, assuming that SSM reaches the blood and stays intact after SC administration, as PGC does. This would give both formulations an additional advantage over unformulated VIP, as it will further increase the concentration of VIP in the inflammation site.

Based on the theoretical considerations illustrated in Fig. 7, strong binding of VIP to the carrier should prevent VIP from extravasation across normal vessels. Thus, the VIP dose that causes a significant decrease in blood pressure should be greatly increased with formulation compared to unformulated VIP. Binding to the carriers should also have a positive impact on the VIP toxicity that is mediated by the drop in blood pressure. However, a direct comparison of MTDs corresponding to formulated and unformulated VIP is misleading; the MTD of unformulated VIP is very high because the time exposure to the drug is minimal due to the short half-life. It is likely that the protection of VIP in the nanocarrier formulations, together with the formulations providing a constant reservoir of free VIP, multiplies VIP's *in vivo* potency leading to a much lower acute MTD. Therefore, by formulating VIP with PGC or SSM one could potentially also achieve an increase of the therapeutic effect of VIP.

Nanocarrier formulations with lower loading percentage contain less free VIP at the thermodynamic equilibrium so

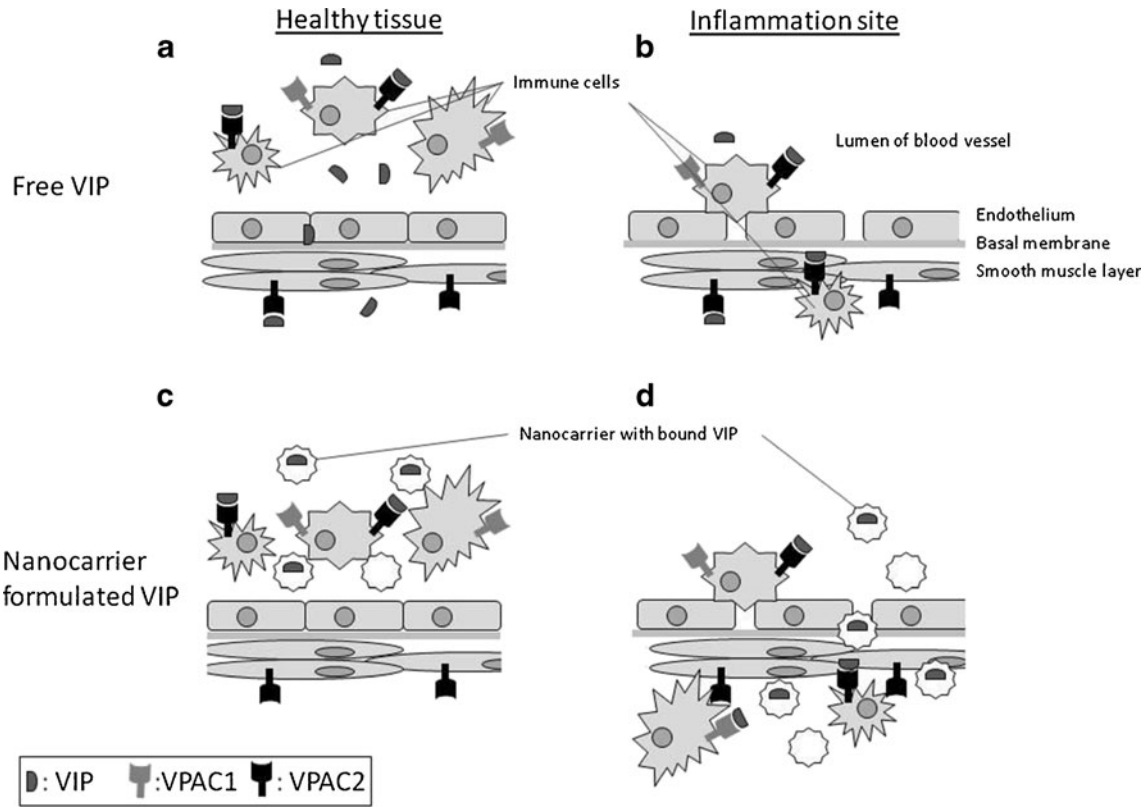

Fig. 7 Free VIP can cross the endothelium and basal membrane in healthy tissue to bind to VPAC2 on perivascular smooth muscle cells thus inducing a profound drop in arterial blood pressure (**a**). It also binds to VPAC 1 and VPAC 2 on immune cells, both in the vascular lumen and at the inflammation site (**b**). If VIP is formulated using a nanocarrier (SSM or PGC) that is too large to penetrate the endothelium in healthy tissue, very little of free VIP is available in the perivascular smooth muscle cell layer to induce a blood pressure decrease (**c**). In inflammation sites, the nanocarrier can extravasate to create a reservoir of bound VIP. This reservoir releases free VIP then free VIP binds to the VPAC1 and VPAC2 receptors on immune cells, which have higher VIP binding affinity than the nanocarriers (**d**). If the inflammation is localized, binding of VIP to perivascular smooth muscle cells does not lead to a systemic decrease of blood pressure.

an inverse correlation between loading percentage and MTD is to be expected. The same is true for VIP loading percentage and a VIP dose that causes a significant decrease in arterial blood pressure. Therefore we expected that MTD and the dose corresponding to a significant decrease in blood pressure to be higher for the PGC formulation at low loading percentages, compared to the SSM formulation with the same loading percentage. However, there is a decrease in the MTD for PGC-formulated VIP at loading percentages between 0.75% and 1% while at higher loading percentages the MTD is higher with SSM formulations compared to PGC. The amount of free VIP measured *in vitro* does not account for the above effect. This effect is likely caused by the lower K_d of SSM-VIP complex, while at lower loading percentages with inherently more VIP sequestered in the carrier, the carrier stability might play a bigger role. It appears that SSM-VIP and PGC-VIP formulations release VIP differently as the MTD decreases more gradually with SSM formulations compared to PGC.

A good compromise between acute MTD and carrier use was established for both carriers at 0.5% loading. This loading percentage is within the upper plateau of the acute MTD for both carriers. Chronic toxicity was therefore determined at this loading percentage at a dose of 50% of the acute MTD for both carriers. The fact that no significant differences were found in a number of blood chemistry and cardiotoxicity parameters as well as body weight changes after several weeks of multiple daily doses (Tables III–V) demonstrates that both formulations are very safe. Based on the efficacy data in mice (5) and allometric extrapolation, we anticipate that the human dose of VIP is in the range of 1–5 μg/kg. At 0.5% loading of the carriers with VIP the anticipated human dose is more than 100 times lower than the acute MTD for SSM-VIP (625 μg/kg) and more than 250 times lower than the acute MTD for PGC-VIP (1250 μg/kg). Also, our research suggests that if nanocarrier-VIP formulations indeed increase the therapeutic effect of VIP, a human dose of VIP could be considerably reduced with no concomitant loss of therapeutic efficacy.

CONCLUSION

VIP binds to PGC or SSM resulting in formulations with either moderate (PGC) or strong binding (SSM) to the carrier. The formulations improved PK profiles and significantly reduced the drop in blood pressure in experimental animals compared to unformulated VIP. PGC nanocarrier excipient showed a significant improvement of VIP *in vivo* profiles at 0.5% loading (w/w) in comparison to the SSM-based formulation in terms of PK value and toxicity. Thus, PGC-VIP is a good candidate for preclinical studies in various models of inflammatory diseases and serves as an example of the use of PGC as an excipient to enable and improve other injectable peptide formulations.

ACKNOWLEDGMENTS AND DISCLOSURES

The work described in this paper was supported, in part, by NIH SBIR grant 1R43AI082723 and by VA Merit Review.

The NIH had no influence on our decision about study design; the collection, analysis, and interpretation of data; the writing of the report; and the decision to submit the paper for publication.

DCB and AB are consultants to, and ANA, CCJ, GMC, SR, and EMB are employees of PharmaIN Corp.

REFERENCES

1. Said SI, Mutt V. Isolation from porcine-intestinal wall of a vasoactive octacosapeptide related to secretin and to glucagon. Eur J Biochem. 1972;28(2):199–204.
2. Linder S, *et al.* Structure and expression of the gene encoding the vasoactive intestinal peptide precursor. Proc Natl Acad Sci U S A. 1987;84(2):605–9.
3. Bogdanov Jr AA, *et al.* Protected graft copolymer (PGC) in imaging and therapy: a platform for the delivery of covalently and non-covalently bound drugs. Theranostics. 2012;2(6):553–76.
4. Castillo GM, Reichstetter S, Bolotin EM. Extending residence time and stability of peptides by protected graft copolymer (PGC) excipient: GLP-1 example. Pharm Res. 2012;29(1):306–18.
5. Delgado M, *et al.* Vasoactive intestinal peptide prevents experimental arthritis by downregulating both autoimmune and inflammatory components of the disease. Nat Med. 2001;7(5):563–8.
6. Gonzalez-Rey E, *et al.* Vasoactive intestinal peptide induces CD4+, CD25+ T regulatory cells with therapeutic effect in collagen-induced arthritis. Arthritis Rheum. 2006;54(3):864–76.
7. Juarranz Y, *et al.* Protective effect of vasoactive intestinal peptide on bone destruction in the collagen-induced arthritis model of rheumatoid arthritis. Arthritis Res Ther. 2005;7(5):R1034–45.
8. Williams RO. Therapeutic effect of vasoactive intestinal peptide in collagen-induced arthritis. Arthritis Rheum. 2002;46(1):271–3.
9. Delgado M, *et al.* Vasoactive intestinal peptide (VIP) and pituitary adenylate cyclase-activation polypeptide (PACAP) protect mice from lethal endotoxemia through the inhibition of TNF-alpha and IL-6. J Immunol. 1999;162(2):1200–5.
10. Chorny A, Delgado M. Neuropeptides rescue mice from lethal sepsis by down-regulating secretion of the late-acting inflammatory mediator high mobility group box 1. Am J Pathol. 2008;172(5):1297–307.
11. Li H, *et al.* Vasoactive intestinal polypeptide suppressed experimental autoimmune encephalomyelitis by inhibiting T helper 1 responses. J Clin Immunol. 2006;26(5):430–7.
12. Fernandez-Martin A, *et al.* Vasoactive intestinal peptide induces regulatory T cells during experimental autoimmune encephalomyelitis. Eur J Immunol. 2006;36(2):318–26.
13. Gonzalez-Rey E, *et al.* Therapeutic effect of vasoactive intestinal peptide on experimental autoimmune encephalomyelitis: down-regulation of inflammatory and autoimmune responses. Am J Pathol. 2006;168(4):1179–88.
14. Delgado M, *et al.* VIP and PACAP induce shift to a Th2 response by upregulating B7.2 expression. Ann N Y Acad Sci. 2000;921:68–78.
15. Chorny A, Gonzalez-Rey E, Delgado M. Regulation of dendritic cell differentiation by vasoactive intestinal peptide: therapeutic applications on autoimmunity and transplantation. Ann N Y Acad Sci. 2006;1088:187–94.

16. Chorny A, *et al.* Signaling mechanisms of vasoactive intestinal peptide in inflammatory conditions. Regul Pept. 2006;137(1–2):67–74.
17. Fernandez-Martin A, *et al.* VIP prevents experimental multiple sclerosis by downregulating both inflammatory and autoimmune components of the disease. Ann N Y Acad Sci. 2006;1070:276–81.
18. Gonzalez-Rey E, Delgado M. Vasoactive intestinal peptide and regulatory T-cell induction: a new mechanism and therapeutic potential for immune homeostasis. Trends Mol Med. 2007;13(6):241–51.
19. Gomariz RP, *et al.* Regulation of TLR expression, a new perspective for the role of VIP in immunity. Peptides. 2007;28(9):1825–32.
20. Domschke S, *et al.* Vasoactive intestinal peptide in man: pharmacokinetics, metabolic and circulatory effects. Gut. 1978;19(11):1049–53.
21. Conti A, *et al.* Vasoactive intestinal polypeptide and dopamine: effect on prolactin secretion in normal women and patients with microprolactinomas. Neuroendocrinology. 1987;46(3):241–5.
22. Spadaro AC, *et al.* A convenient manual trinitrobenzenesulfonic acid method for monitoring amino acids and peptides in chromatographic column effluents. Anal Biochem. 1979;96(2):317–21.
23. Lapidot Y, Rappoport S, Wolman Y. Use of esters of N-hydroxysuccinimide in the synthesis of N-acylamino acids. J Lipid Res. 1967;8(2):142–5.
24. Ashok B, *et al.* Effects of peptide molecular mass and PEG chain length on the vasoreactivity of VIP and PACAP(1-38) in pegylated phospholipid micelles. Peptides. 2004;25(8):1253–8.
25. Lim SB, Rubinstein I, Onyuksel H. Freeze drying of peptide drugs self-associated with long-circulating, biocompatible and biodegradable sterically stabilized phospholipid nanomicelles. Int J Pharm. 2008;356(1–2):345–50.
26. Castillo GM, *et al.* Sulfate content and specific glycosaminoglycan backbone of perlecan are critical for perlecan's enhancement of islet amyloid polypeptide (amylin) fibril formation. Diabetes. 1998;47(4):612–20.
27. Castillo GM, *et al.* Perlecan binds to the beta-amyloid proteins (A beta) of Alzheimer's disease, accelerates A beta fibril formation, and maintains A beta fibril stability. J Neurochem. 1997;69(6):2452–65.
28. Talke H, Schubert GE. Enzymatic urea determination in the blood and serum in the Warburg optical test. Klin Wochenschr. 1965;43:174–5.
29. Larsen K. Creatinine assay by a reaction-kinetic principle. Clin Chim Acta. 1972;41:209–17.
30. Foster PW, Rick JJ, Wolfson WQ. Studies in serum proteins. VI. The extension of the standard biuret method to the estimation of total protein in urine. J Lab Clin Med. 1952;39(4):618–23.
31. Goa J. A micro biuret method for protein determination; determination of total protein in cerebrospinal fluid. Scand J Clin Lab Invest. 1953;5(3):218–22.
32. Sister Mary W, Hess WC. A comparison of total serum protein and albumin values as determined by the micro-Kjeldahl, Biuret, and Folin methods. Bull Georgetown Univ Med Cent. 1952;6(2):34–5.
33. Drupt F, *et al.* Serum albumin assay by bromocresol green method: application to different automatic apparatus. Ann Pharm Fr. 1974;32(5):249–56.
34. Rasanayagam LJ, *et al.* Measurement of urine albumin using bromocresol green. Clin Chim Acta. 1973;44(1):53–7.
35. Webster D, Bignell AH, Attwood EC. An assessment of the suitability of bromocresol green for the determination of serum albumin. Clin Chim Acta. 1974;53(1):101–8.
36. Bergmeyer HU, Scheibe P, Wahlefeld AW. Optimization of methods for aspartate aminotransferase and alanine aminotransferase. Clin Chem. 1978;24(1):58–73.
37. Henry RJ, *et al.* Revised spectrophotometric methods for the determination of glutamic-oxalacetic transaminase, glutamic-pyruvic transaminase, and lactic acid dehydrogenase. Am J Clin Pathol. 1960;34:381–98.
38. Mullon CJ, Langer R. Determination of conjugated and total bilirubin in serum of neonates, with use of bilirubin oxidase. Clin Chem. 1987;33(10):1822–5.
39. Arleth L, *et al.* Detailed structure of hairy mixed micelles formed by phosphatidylcholine and PEGylated phospholipids in aqueous media. Langmuir. 2005;21(8):3279–90.
40. Sato T, *et al.* Poly(ethylene glycol)-conjugated phospholipids in aqueous micellar solutions: hydration, static structure, and interparticle interactions. J Phys Chem B. 2007;111(6):1393–401.
41. Onoue S, Yamada S, Yajima T. Bioactive analogues and drug delivery systems of vasoactive intestinal peptide (VIP) for the treatment of asthma/COPD. Peptides. 2007;28(9):1640–50.
42. Petkov V, *et al.* The vasoactive intestinal peptide receptor turnover in pulmonary arteries indicates an important role for VIP in the rat lung circulation. Ann N Y Acad Sci. 2006;1070:481–3.
43. Petkov V, *et al.* Vasoactive intestinal peptide as a new drug for treatment of primary pulmonary hypertension. J Clin Invest. 2003;111(9):1339–46.
44. Sethi V, Onyuksel H, Rubinstein I. Liposomal vasoactive intestinal peptide. Methods Enzymol. 2005;391:377–95.
45. Jarhult J, Hellstrand P, Sundler F. Immunohistochemical localization and vascular effects of vasoactive intestinal polypeptide in skeletal muscle of the cat. Cell Tissue Res. 1980;207(1):55–64.
46. Gomariz RP, *et al.* VIP-PACAP system in immunity: new insights for multitarget therapy. Ann N Y Acad Sci. 2006;1070:51–74.
47. Laburthe M, Couvineau A, Tan V. Class II G protein-coupled receptors for VIP and PACAP: structure, models of activation and pharmacology. Peptides. 2007;28(9):1631–9.
48. Maeda H, *et al.* Tumor vascular permeability and the EPR effect in macromolecular therapeutics: a review. J Control Release. 2000;65(1–2):271–84.
49. Caliceti P, Veronese FM. Pharmacokinetic and biodistribution properties of poly(ethylene glycol)-protein conjugates. Adv Drug Deliv Rev. 2003;55(10):1261–77.
50. Torchilin V. Lipid-Core Micelles for Target Drug Deliv. 2005.
51. Torchilin VP. Block copolymer micelles as a solution for drug delivery problems. Expert Opinion on Therapeutic Patents. 2005;15(1):63–75.
52. Supersaxo A, Hein WR, Steffen H. Effect of molecular weight on the lymphatic absorption of water-soluble compounds following subcutaneous administration. Pharm Res. 1990;7(2):167–9.
53. Chorny A, *et al.* Vasoactive intestinal peptide induces regulatory dendritic cells with therapeutic effects on autoimmune disorders. Proc Natl Acad Sci U S A. 2005;102(38):13562–7.
54. Chorny A, *et al.* Vasoactive intestinal peptide generates CD4+ CD25+ regulatory T cells in vivo: therapeutic applications in autoimmunity and transplantation. Ann N Y Acad Sci. 2006;1070:190–5.
55. Delgado M. Inhibition of interferon (IFN) gamma-induced Jak-STAT1 activation in microglia by vasoactive intestinal peptide: inhibitory effect on CD40, IFN-induced protein-10, and inducible nitric-oxide synthase expression. J Biol Chem. 2003;278(30):27620–9.
56. Delgado M, Ganea D. Vasoactive intestinal peptide inhibits IL-8 production in human monocytes by downregulating nuclear factor kappaB-dependent transcriptional activity. Biochem Biophys Res Commun. 2003;302(2):275–83.
57. Delgado M, *et al.* Vasoactive intestinal peptide and pituitary adenylate cyclase-activating polypeptide stimulate the induction

of Th2 responses by up-regulating B7.2 expression. J Immunol. 1999;163(7):3629–35.
58. Delgado M, *et al.* VIP and PACAP inhibit IL-12 production in LPS-stimulated macrophages. Subsequent effect on IFNgamma synthesis by T cells. J Neuroimmunol. 1999;96 (2):167–81.
59. Gonzalez-Rey E, *et al.* Vasoactive intestinal peptide generates human tolerogenic dendritic cells that induce CD4 and CD8 regulatory T cells. Blood. 2006;107(9):3632–8.
60. Gonzalez-Rey E, Delgado M. Therapeutic treatment of experimental colitis with regulatory dendritic cells generated with vasoactive intestinal peptide. Gastroenterology. 2006;131 (6):1799–811.
61. Gutierrez-Canas I, *et al.* VIP down-regulates TLR4 expression and TLR4-mediated chemokine production in human rheumatoid synovial fibroblasts. Rheumatology (Oxford). 2006;45 (5):527–32.
62. Juarranz MG, *et al.* Vasoactive intestinal peptide modulates proinflammatory mediator synthesis in osteoarthritic and rheumatoid synovial cells. Rheumatology (Oxford). 2004;43(4):416–22.
63. Juarranz Y, *et al.* VIP decreases TLR4 expression induced by LPS and TNF-alpha treatment in human synovial fibroblasts. Ann N Y Acad Sci. 2006;1070:359–64.
64. Larocca L, *et al.* VIP limits LPS-induced nitric oxide production through IL-10 in NOD mice macrophages. Int Immunopharmacol. 2007;7(10):1343–9.
65. Martinez C, *et al.* Vasoactive intestinal peptide and pituitary adenylate cyclase-activating polypeptide modulate endotoxin-induced IL-6 production by murine peritoneal macrophages. J Leukoc Biol. 1998;63(5):591–601.
66. Tao Q, Ren J, Li J. Vasoactive intestinal peptide inhibits adhesion molecule expression in activated human colon serosal fibroblasts by preventing NF-kappaB activation. J Surg Res. 2007;140(1):84–9.